Multimedia Tools and Applications (2021) 80:2565–2582
https://doi.org/10.1007/s11042-020-09646-3

Blood vessel segmentation and extraction using H-minima method based on image processing techniques

Salma M. Boubakar Khalifa Albargathe[1] **· Ersin Kamberli**[2] **· Fatma Kandemirli**[2] **· Javad Rahebi**[3]

Received: 9 September 2019 / Revised: 24 July 2020 / Accepted: 18 August 2020 /
Published online: 15 September 2020

Abstract
In this paper, the H-minima transform is used for blood vessel segmentation. The aim of this study is to get the high accuracy of blood vessel segmentation in retinal images. In this study the good result and good performance were got. We compared our result with other methods. Also for simulation result we implemented on DRIVE and STARE database. The proposed method shows very remarkable performance on pathological retinal images. For the implementing of the proposed method MATLAB 2019a software is used. The running time of this method was 1 s for each image and the average accuracy for STARE dataset and DRIVE dataset achieved to 0.9591 and 0.9672 respectively.

Keywords Fundus camera · Image processing · Retina image

✉ Ersin Kamberli
ekamberli@kastamonu.edu.tr

Salma M. Boubakar Khalifa Albargathe
albragate83@yahoo.com

Fatma Kandemirli
fatma@kastamonu.edu.tr

Javad Rahebi
cevat.rahebi@altinbas.edu.tr

[1] Department of Material Science and Engineering, Kastamonu University, Kastamonu, Turkey

[2] Department of Biomedical Engineering, Kastamonu University, Kastamonu, Turkey

[3] Department of Electrical and Computer Engineering, Altinbas University, Istanbul, Turkey

1 Introduction

In addition to technological development, significant progress and a number of advances have been recorded in the computer techniques used in medical applications. Automatic image processing and analysis are widely used in the area of medical diagnosis and treatment. Recent developments in the field of medical image processing in particular enable the automatic detection of various characteristics, changes, diseases and degenerative problems via retinal images. Retinal image analyses use image processing techniques and is aimed at determining and monitoring diseases that can be detected via changes in the structure of the retina.

Nguyen et al. [15] proposed a blood vessel segmentation method that uses multiscale line detection. The proposed method is based on changing the length of the line detector and as a result of this process various line detector with different measurements are gathered. To preserve the efficiency of this method while eliminating the cons of every individual line detector, the final segmentation of every retinal image is produced by varying measurements that are linearly joint. The performance this method was evaluated on 3 databases that avowedly available, these databases are DRIVE, STARE and REVIEW. The proposed method achieves high accuracy on DRIVE and STARE databases compared to other existing methods. The accuracy for DRIVE is 0.9407 and for STARE it is 0.9324.These result was gathered where the density of vessels is high and hard to make segmentation. This method produces an accurate segmentation process on the central reflex vessel and it can be verified by visual inspection.

On the other hand the performance on REVIEW database is also immensely proper and close to the measurement that supplied by experts. Additionally the proposed method has lots of advantages like; quick segmentation tense, primitiveness and stability to overcome with retinal images that has high resolutions.

Roychowdhury et al. [19] proposed a method for segmentation of blood vessels based on major vessel extraction and additionally sub-image classification. The proposed method presents a new three staged blood vessel segmentation algorithm with using fundus images. On the initial step the green plane of fundus picture is accumulated and this picture is pre-handled to remove a paired picture directly after high pass sifting and what's more the other double picture for the vessel areas is upgraded by morphological reproduction. Major vessel regions are specified as the intersection between threshold version of pre-processed retinal images like top-hat image and filtered image. The regions common to both high passed filter and morphologically reconstructed images are ejected as major veins. The number of pixels that specified as major vessels can be either increased or decreased with varying the pixel threshold value. Furthermore all of the residual pixels from both binary images are classified with the aid of a Gaussian Mixture Model (GMM). After that a Gaussian Mixture Model classifier with 2-Gaussian is used for identifying the decent vessel pixels. This classifier uses a set of 8 features. These 8 features are extracted from neighbor pixel and first-second order gradient images. Subsequently the major parts of vessels will be combined with the classified vessel pixels. This proposed method requires short segmentation time while achieving well accuracy on retinal images. The accuracy of this proposed method is %95.2. This method was tested on 3 avowedly available datasets, DRIVE, STARE and CHASE_DB1. This proposed method outperforms nearly most of the existing methods. Additionally required segmentation time of this method is approximately 8 s. The proposed method by Marin et al. [14] requires a time of 90 s to complete the process, while this proposed method by Roychowdhury et al. [19] needs one in ten time compared to Marin's method. Ranjit Ghoshal et al. used mathematical morphological operation for retinal vessel extraction [6]. In their method they used new Structure-measure.

Retinal blood vessel segmentation by Deep learning methods proposed in [4, 13, 16]. Deep supervised method is proposed in [7]. Lam et al. [12] proposes a vessel division procedure utilizing regularization and in view of multi concavity displaying. Recognizing vein in retinal pictures that has shiny and dim sores is a testing undertaking. To overcome this problem this proposed method uses multi concavity modeling. This method used both line-shaped concavity measurement and differentiable concavity measurement. The task of differentiable concavity measurement is handling the shiny lesions while line-shaped concavity measurement is handling the dim lesions which have diverse intensity structure from vessels in retinal images that has line shape. Since the shiny lesions have an excessive intensity, bright lesion can be effectively separated from both vessel and non-vessels with measuring the concavity degree. The blood vessel has a line shaped intensity structure while dim lesions have an unsteady shape. The line-shape concavity is demonstrated to cut of the dull injury while keeping up the locales of veins. To manage shoddily appropriated commotion because of different circular power in retinal pictures and normalizing the qualities of the clamor evacuation, the privately standardized concavity measure is outlined. These 3 concavity measures are joined together with a specific end goal to distinguish vessels in retinal pictures. The trial after effects of proposed strategy yields the best execution over existing strategies on distorted retinas and the exactness of this technique is beating the human eyewitness, which has not been accomplished by some other existing strategies yet.

For this paper, the main contributions are as follows:

1) H-minima transformation is used for enhancing the blood vessels.
2) The method that used for Structural element is good.
3) Process time of blood vessels segmentations are very fast.
4) Accuracy of the segmentation is high.

The motivation of the proposed method is use the H-minima transformation to enhancing the blood vessels and also the good scenario to preprocessing.

This paper arranged in 5 sections. In section II the material and methods will present and discuss. In section III the proposed method will discuss. In section IV the performance evaluation and results will present and finally this paper with conclude with the conclusion section.

2 Material and method

2.1 DRIVE database

The DRIVE (Digital Retinal Images for Vessel Extraction) is a publicly available database. The photographs for the DRIVE database were obtained from a diabetic retinopathy screening program in The Netherlands. The screening population consisted of 400 diabetic subjects between 25 and 90 years of age. Forty photographs have been randomly selected, 33 do not show any sign of diabetic retinopathy and 7 show signs of mild early diabetic retinopathy. Figure 1 for an example of both a normal and a pathological image [21].

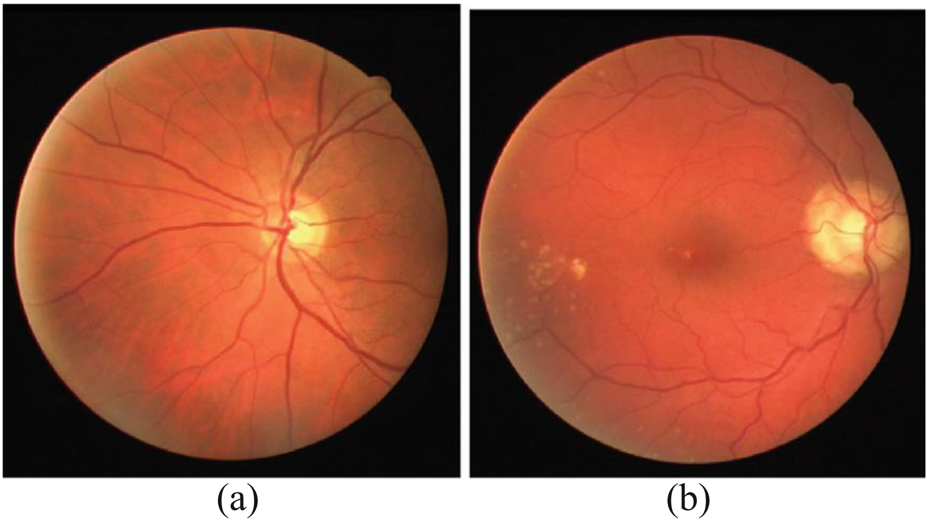

Fig. 1 Retina images from DRIVE: **a** healthy retina **b** retinal pathology

The images were acquired using a Canon CR5 non-mydriatic 3CCD camera with a 45 degree field of view (FOV). Each image was captured using 8 bits per color plane at 768 by 584 pixels. For this database, the images have been cropped around the FOV. For each image, a mask image was provided that delineates the FOV [21]. The set of 40 images has been divided into a training and a test set, both containing 20 images. For the training images, a single manual segmentation of the vasculature is available. For the test cases, two manual segmentations are available; one is used as gold standard, the other one can be used to compare computer generated segmentations with those of an independent human observer. All human observers that manually segmented the vasculature were instructed and trained by an experienced ophthalmologist. All of the images contained in the database were actually used for making clinical diagnoses. The performance of our vessel segmentation algorithm was measured on the test set using the segmentation of set X as a ground truth. Figure 2 shows an example of retinal fundus image of DRIVE database and the related ground truth and FOV mask for corresponding image.

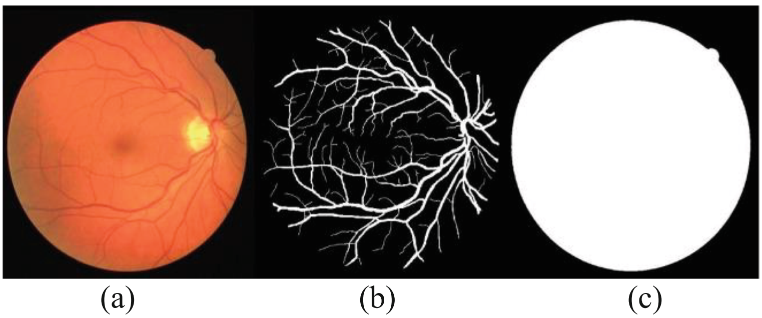

Fig. 2 Retinal fundus image 02 from test set of the DRIVE database. **a** Original RGB image **b** manual segmentation of blood vessels known as a ground truth **c** the FOV mask of the corresponding image

2.2 STARE database

The STARE (STructured Analysis of the Retina) is a publicly available database contains 20 images for segmentation of blood vessels, 10 of which are pathological images. Figure 3 shows retina images from the STARE database.

The field of view was drawn using a Canon TRV-50 fundus camera with 35 degrees (FOV). The resolution of the captured images is 605 × 700, and each image area was cropped to obtain images at a resolution of 650 × 500 including a diameter circle [8, 9]. Two observers manually segmented all the images. The difference in segmentation between the two observers is due to the fact that the second observer segmented many more of the thinner vessels than the first one. Performance was computed with the segmentation of the first observer as the ground truth.

2.3 H-minima

H-minima transform is the method proposed to replace the Wolf pruning [23]. H-minima transform suppresses all regional minima in I, whose depth is less than or equivalent to H. I is the areal surface topography dataset, while H is the height threshold value (non-negative scalar) [18].

To eliminate all regional minima, except the significant minima, H-minima transforms can be applied to specify a height threshold value by using the following equation:

$$H = N*Z \tag{1}$$

Where:

H Limit of Height.
Z maximum distance from mean plane.
N Percentage of Maximum Height (%).

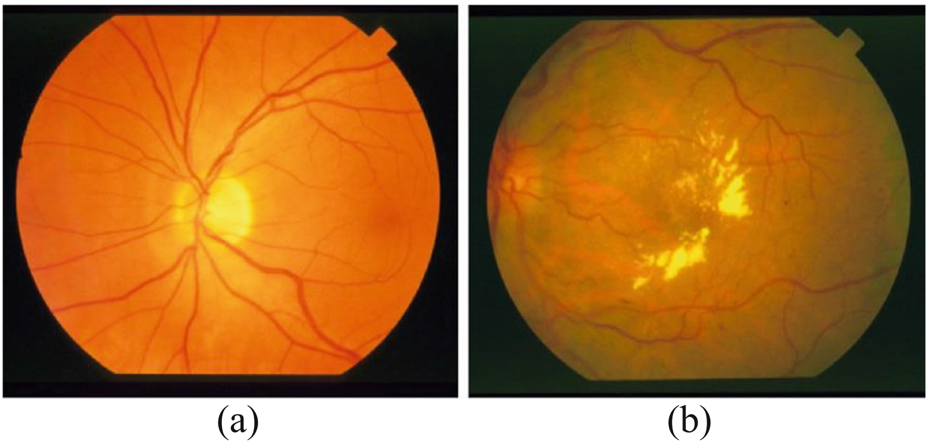

Fig. 3 Retina Images from STARE: **a** healthy retina, **b** pathological retina

While considering the equation 3.4, it can be observed the threshold value of height (H) is depending on the percentage of the Maximum height. Value of N can show a difference of 5% to 20% depending on the disorders of the restrained plane topography [10].

H-minima is an image analysis technique used on MATLAB [24]. The "imhmin" command is used for processing H-minima technique." imhmin(I,h)" command compresses the all minima in the intensity image which has a depth value of h. The intensity image can be showed as I and additionally h values must be a scalar. The connected components of the pixels which has a stationary intensity value are called Regional minima by default, "imhmin" command will use 8-connected localities for 2 dimension pictures, and 26-connected localities for 3 dimension images [24].

3 The proposed method

The summary of the proposed method is shown in Fig. 4.

The steps of this flow chart are as following steps:

3.1 Read the input image

In this step from the STARE and DRIVE database the image is read by using imread function. The original image, manual segmented and mask are read from DRIVE database. The result of this step is shown in Fig. 5.

3.2 Select green channel

Retina image taken by a fundus camera was converted into a grayscale image in order to make easy computations and decrease the size of data and computational time. Any Color digital images are made of pixels, and pixels are made of combinations of primary colors represented by a series of code. A channel in this context is the grayscale image. An image from a standard digital camera will have a red, green and blue channel. For processing the green channel was selected because green channel has more difference intensity between vessel and non-vessel parts. This scenario is shown in Fig. 6.

As shown in this figure the blood vessel in green channel is clearer than the other channels. For this reason we selected the green channel.

3.3 Contrast enhancement

In this step the contrast enhancement method implemented to increase the contrast. The enhancement methods were used for green channel. Because this channel supports important blood vessel structural information. For enhancement we used the Morphological structuring element that an essential part of the erosion operation on the input image as 'disk' with radius 3 for create a flat structure element in the form of a disk to enhancing the image, as shown in Fig. 7.

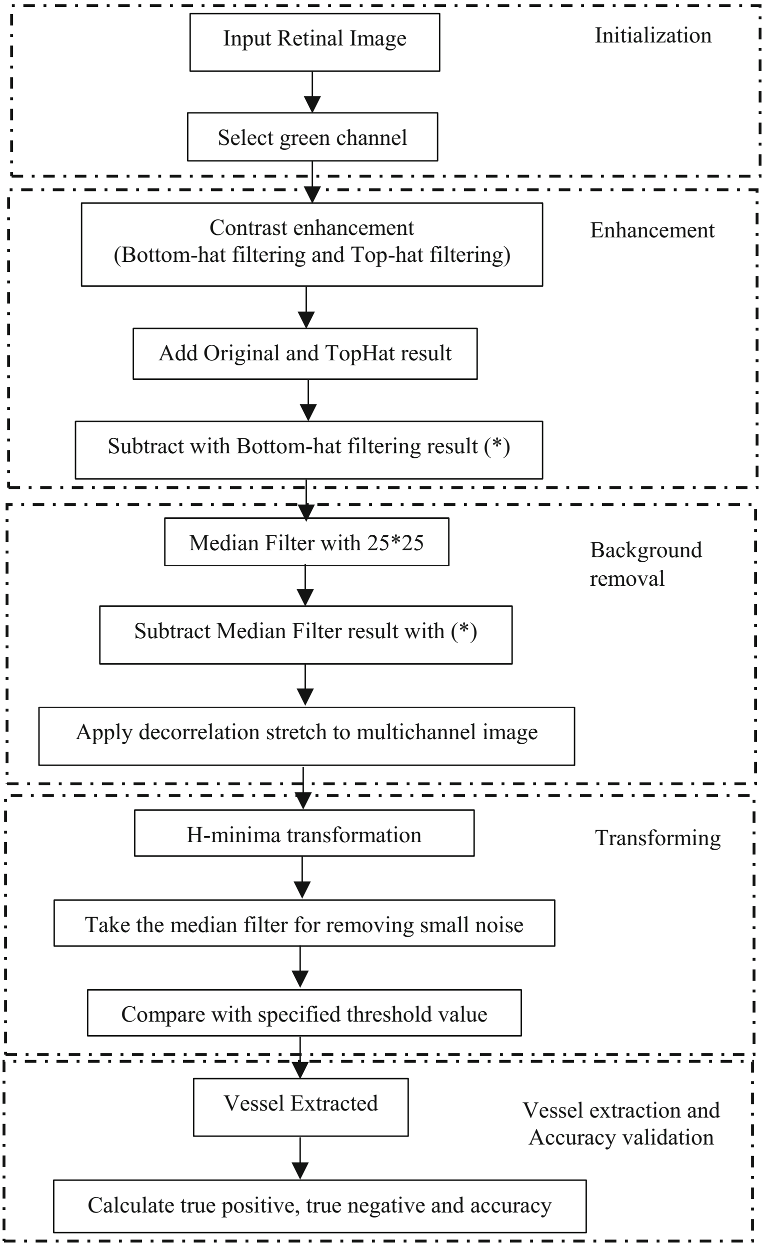

Fig. 4 Summary of the proposed method

We expressed the erosion operation as follows:

$$A \ominus B = \{z \in E | B_z \subseteq A\} \tag{2}$$

Where E be an integer grid, and a binary image in E,Bz is the translation of B by the vector z, When the structuring element B has a center (e.g. a disk), and this center is located on the

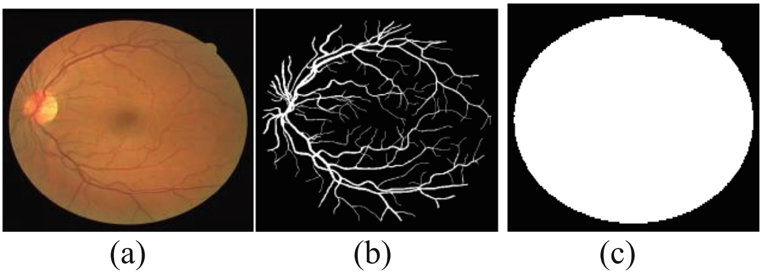

Fig. 5 **a** Original image, **b** manual segmented image, **c** mask

origin of E, then the erosion of A by B can be understood as the locus of points reached by the center of B when B moves inside A [1].

Also we used the Bottom-hat filtering and Top-hat filtering for image enhancement. Bottom-hat filtering is an operation that extracts small elements and details from given images. There exist two types of Top-hat filtering: The white Bottom-hat transform is defined as the difference between the input image and its opening by some structuring element, the white top-hat transform of *f* is given by:

$$\mathrm{Tw}\ (f) = f - f \circ b \tag{3}$$

Where ○ denotes the opening operation, f: E → R be a gray scale image, mapping points from an integer grid E, b be a gray scale structuring element.

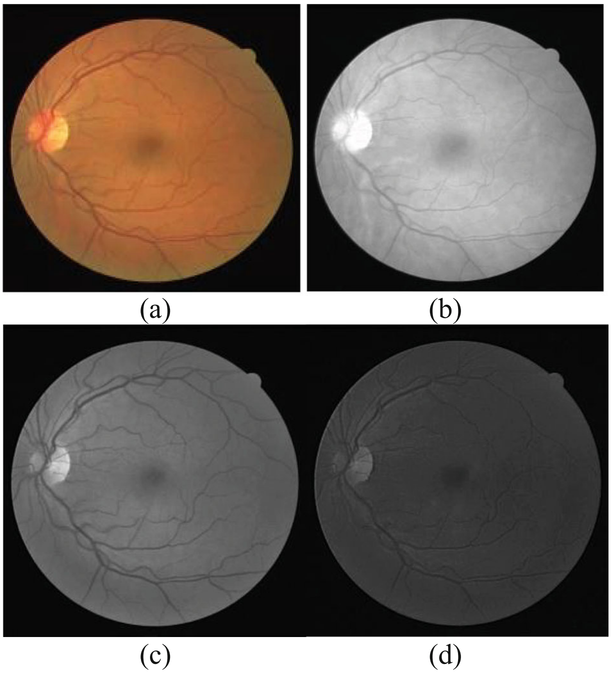

Fig. 6 **a** Original image, **b** Red channel, **c** Green channel, **d** Blue channel

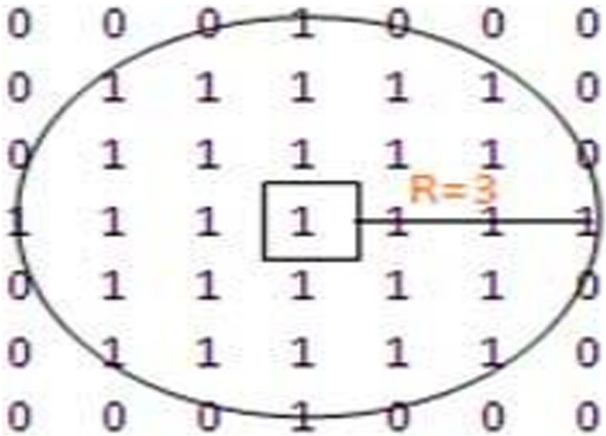

Fig. 7 Structuring element as 'disk' with radius 3

The black Bottom -hat transform is defined dually as the difference between the closing and the input image. The black top-hat transform of f (sometimes called the bottom-hat transform) is given by:

$$Tb\ (f) = f \bullet b - f \tag{4}$$

where • is the closing operation [2].

After applied these methods the result is shown in Fig. 8.

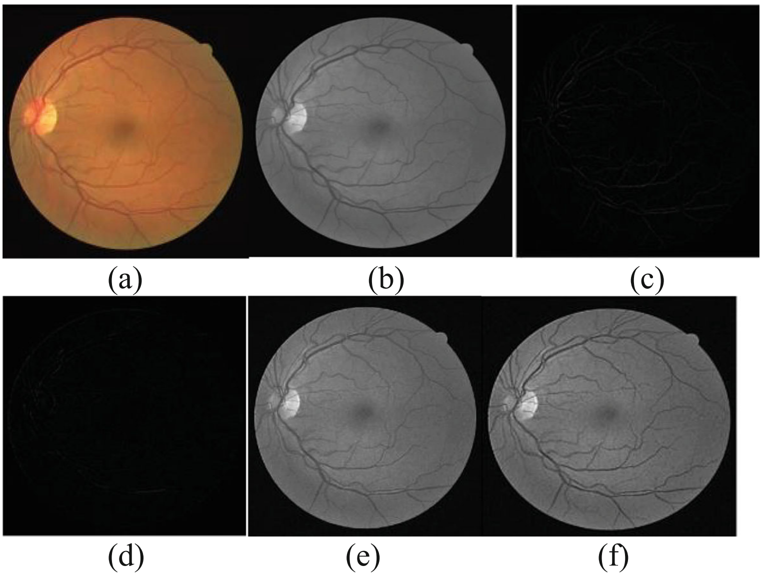

Fig. 8 **a** Original image, **b** Green channel, **c** Bottom-hat filtering **d** Top-Hat filtering **e** Add the original image to the Top-Hat filtered **f** subtract the Bottom-hat filtered from result Fig. 8e)

3.4 Background removal and remove the central light reflex

The high resolution fundus photographs often display a central light reflex. The light reflex of the retinal vessel is formed by the reflection from the interface between the blood column and vessel wall. In this step the preprocessing and Vessel Central Light Removal were done. For getting the foreground the median filter with size 25*25 was used. In other word for smoothing the vessel and non-vessel part the median filter was used. This result is shown in Fig. 9.

We applied decorrelation stretch to multichannel image on result Fig. 10c) for enhance or stretch, color differences found in each pixel of an image. Also used for saturating equal fractions at low and high intensities. This result is illustrated in Fig. 10.

3.5 Median filtering

An image containing salt-and-pepper noise will have dark pixels in bright regions and bright pixels in dark regions so we used median filtering with size 3*3 to reduce "salt and pepper" noise(smoothing). The median filter replaces a pixel by the median, instead of the average, of all pixels in a neighborhood w

$$y[m,n] = median\{x[i,j],(i,j)\in w\} \tag{5}$$

where w represents a neighborhood defined by the user, centered around location [m,n] in the image [22].

This result is shown in Fig. 11.

3.6 Apply the H-minima transformation

We applied H-minima transform to reduce over-segmentation by used imhmin function. This function removes all regional minima in the grayscale image whose depth is less or equal to the given threshold level h, and it increases the depth of the remaining regional minima by the value of h. (A "regional minimum" was defined as a connected component of pixels with an equal pixel value that is less than the value of all its neighboring pixels. And the "depth" of a regional minimum can be thought of as minimum pixel value difference between the regional minimum and its neighboring maxima.)

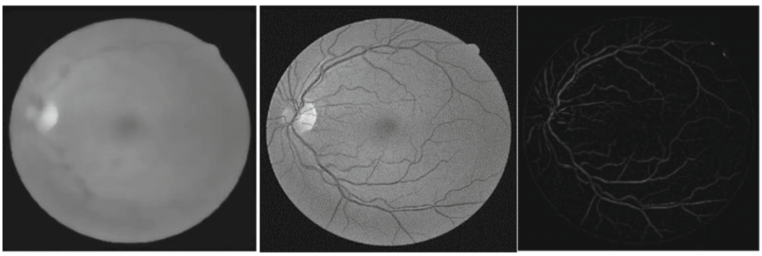

(a) (b) (c)

Fig. 9 **a** Median filter result, **b** ((Original + TopHat) - Bottom-Hat) **c** subtraction of median filter with result b (background removal)

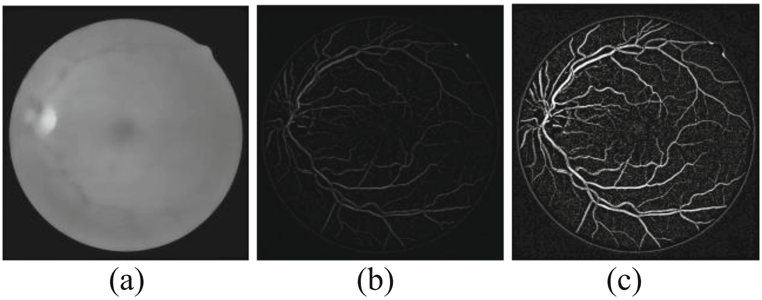

Fig. 10 **a** Median filter result, **b** subtraction of median filter with ((Original + TopHat) - Bottom-Hat) **c** Apply decorrelation stretch to multichannel image on result Fig. 10b

In this study we used the Eq. (9) for calculating the h value [20].

$$\mathrm{h} = \frac{2}{mn}\sqrt{\sum(g{-}g)^2} \tag{6}$$

In this equation m and n is row and column value respectively.g is the pixel intensity and $\overline{g}$ is the average value of$g$.

The result of this step is shown in Fig. 12.

3.7 Thresholding and binarization

Thresholding is a great way to extract useful information encoded into pixels while minimizing background noise. Thresholding methods replace each pixel in an image with a black pixel if the image intensity is less than constant T, or a white pixel if the image intensity is greater than that constant this lead to create binary image divided into two regions:

- Pixel values that are less than or equal to the threshold background.
- Pixel values greater than the threshold foreground (vessels).

Threshold image g(m,n) can be define [11]:

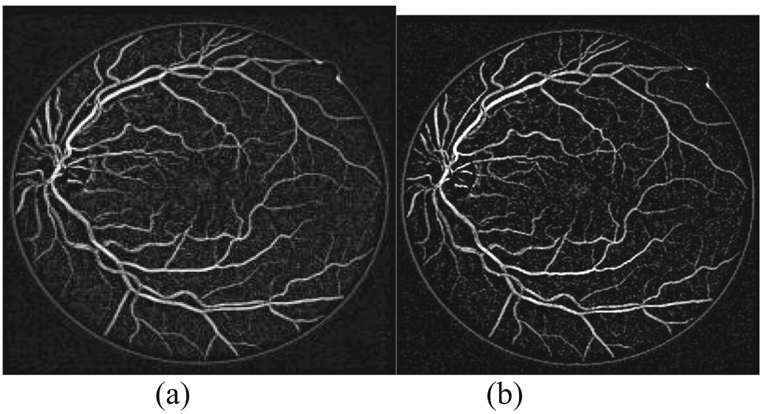

Fig. 11 **a** Before used median filtering, **b** after used median filtering

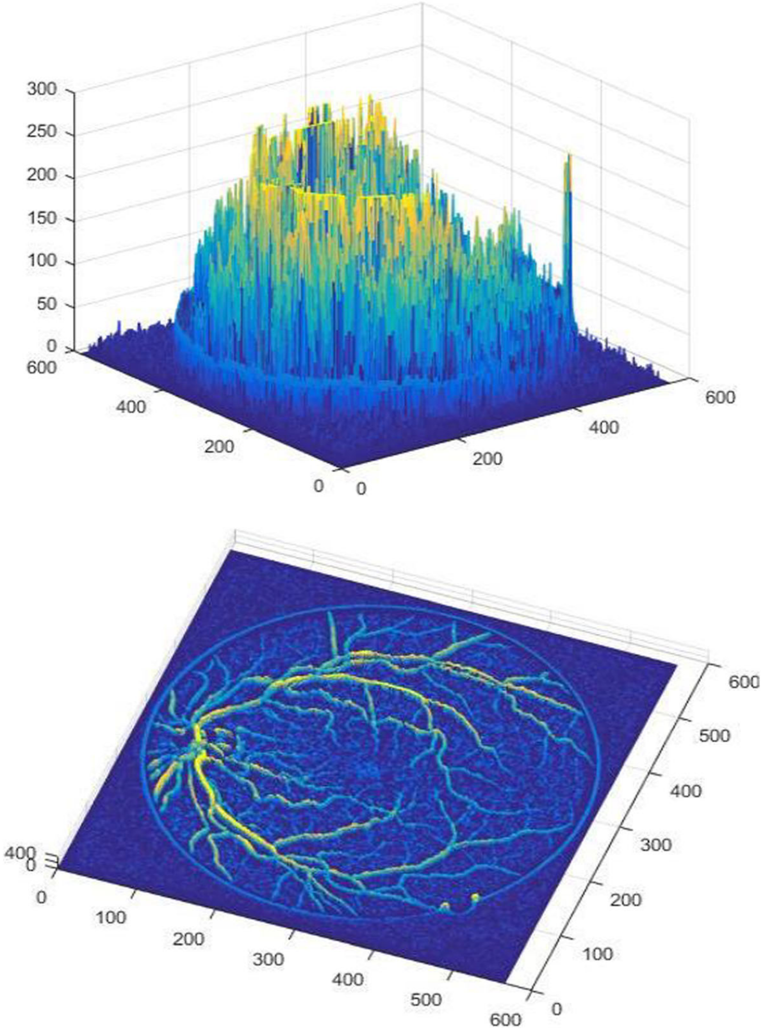

Fig. 12 H-minima transformation result

$$g(m,n) = \begin{cases} 1 & if\ f(m,n) \geq T \\ 0 & O.w. \end{cases} \tag{7}$$

After getting the vessel, these vessels are not exact vessel which the algorithm is seeking the result of this step is shown in Fig. 13b.

For getting high performance the vessel the binarization method was used. The simplest way to use image binarization is to choose a threshold value, and classify all pixels with values above. In this study the robust thresholding was found and selected to get the exact vessels but we had spots noise we used the two morphological operations For removing those spots:

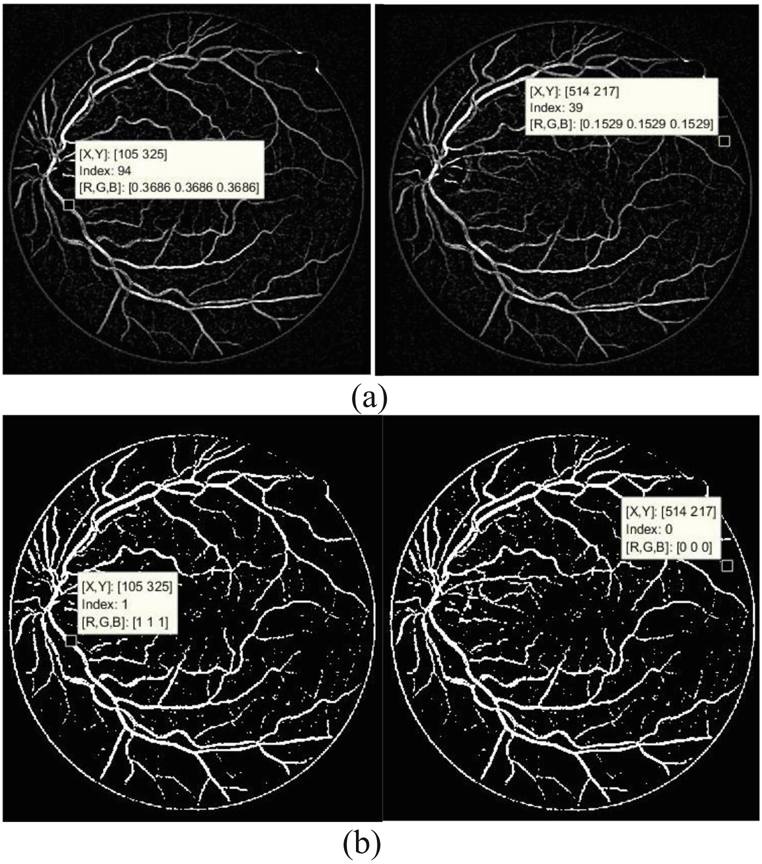

Fig. 13 **a** before used thresholding. **b** After used thresholding

Imclose: Morphological Closing used for fill spots in Images (close small spots between foreground regions). The closing of a set (binary image) A by a structuring element B is the erosion of the dilation of that set is given by:

$$A \bullet B = (AB) \ominus B \tag{8}$$

where □ and denote the dilation and erosion, respectively [1].

- Bwmorph: Morphological operations on binary images used for removing isolated spots in foreground.

Then the result is binarized with this value and then the vessel is got. The final result is shown in Fig. 14.

3.8 Performance measure calculation for segmentation retinal vessel image

Performance measure procedure was done by comparing the segmentation results to the reference image. There are four values resulted from the validation procedure used for

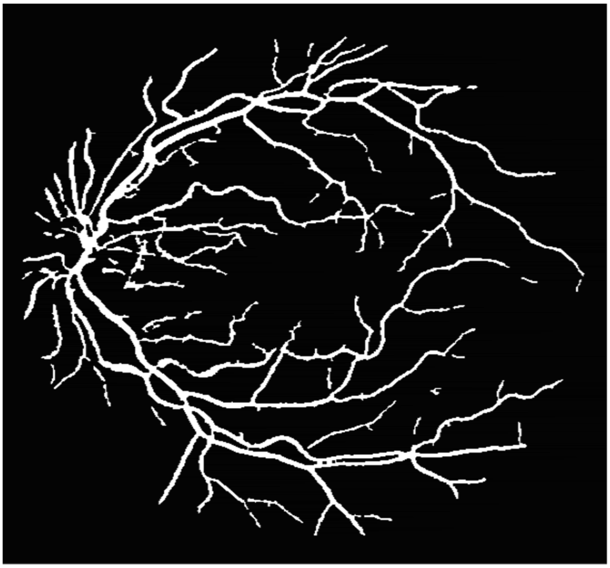

Fig. 14 The Vessel Extracted

performance analyzing the true positive, true negative, false positive and false negative were analyzed and calculated. Also sensitivity and specificity and accuracy were calculated.

4 Performance evaluation and results

There are several terms that are commonly used along with the description of sensitivity, specificity and accuracy [3].

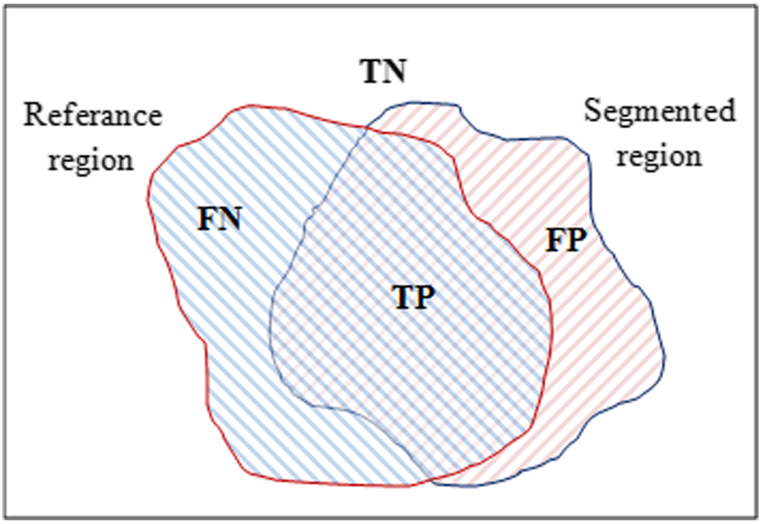

Fig. 15 Sensitivity, Specificity and Accuracy [17]

In the retinal vessel segmentation process, the outcome is a pixel-based classification result. Any pixel is classified either as vessel or surrounding tissue. Consequently, there are four possibilities; two classifications and two misclassifications. The classifications are the true positive (TP) where a pixel is identified as vessel in both the ground truth and segmented image, and the true negative (TN) where a pixel is classified as a non-vessel in the ground truth and the segmented image. The two misclassifications are the false negative (FN) where a pixel is classified as non-vessel in the segmented image but as a vessel pixel in the ground truth image, and the false positive (FP) where a pixel is marked as vessel in the segmented image but non-vessel in the ground truth image. All this situations are shown in Fig. 15.

TPR and FPR illustration; TP indicates positive pixels which have correctly been labeled positive, FP indicates incorrect negative pixels which have been labeled positive, FN indicates positive pixels which have incorrectly been labeled as negative pixels and TN indicates negative pixels which have correctly been labeled as negative. If a disease is proven present in a patient, the given diagnostic test also indicates the presence of disease, the result of the diagnostic test is considered true positive (TP). If a disease is proven absent in a patient, the diagnostic test suggests the disease is absent as well, the test result is true negative (TN). Both (TP) and (TN) suggest a consistent result between the diagnostic test and the proven condition (also called standard of truth). However, no medical test is perfect. If the diagnostic test indicates the presence of disease in a patient who actually has no such disease, the test result is false positive (FP) [17]. Crossing and branching in the veneer can complicate the image model. Most medical images pose significant problems in removing blood vessels, such as signal noise, image intensity shift, and image contrast mishandling [5].

The sensitivity (TPR), specificity (TNR) and accuracy (ACC) are shown as Eqs. (9), (10) and (11) respectively.

$$\text{Sensitivity (TPR)} = \text{TP}/(\text{TP} + \text{FN}) \tag{9}$$

$$\text{Specificity (TNR)} = \text{TN}/(\text{TN} + \text{FP}) \tag{10}$$

$$\text{Accuracy (ACC)} = (\text{TP} + \text{TN})/(\text{TP} + \text{FN} + \text{TN} + \text{FP}) \tag{11}$$

The result for STARE database is shown in Table 1.

The comparison between results of accuracy, specificity and sensitivity for DRIVE database is shown in Fig. 16.

The Comparison of the result for DRIVE (train) is shown in Fig. 17.

The comparison between results of accuracy, specificity and sensitivity for STARE is shown in Fig. 18.

5 Conclusion

In this study, we used unsupervised method to subtract the vessels in the retina, based on H-minima Transformation algorithm was proposed to accurately extract the vessels from the retinal images, taking into consideration the features of retinal images. First, some preprocessing has been applied to the images. To do this, the best sub-bands of color images were initially chosen. We then corrected the brightness changes in the retinal images by applying the

Table 1 Result for STARE database

Image number	Specificity	Sensitivity	Accuracy
1	0.961542	0.733868	0.943372
2	0.969881	0.645985	0.948309
3	0.948528	0.822924	0.941011
4	0.965201	0.70852	0.946172
5	0.974203	0.712445	0.950557
6	0.979404	0.736981	0.962519
7	0.978971	0.841637	0.967965
8	0.97488	0.834794	0.964423
9	0.979231	0.822396	0.966895
10	0.965335	0.783304	0.950697
11	0.983568	0.809443	0.971159
12	0.983698	0.866019	0.974597
13	0.97865	0.780404	0.961001
14	0.982521	0.772002	0.963452
15	0.979751	0.73922	0.95898
16	0.985481	0.603057	0.946432
17	0.990539	0.76614	0.970456
18	0.99224	0.68998	0.976954
19	0.97903	0.766511	0.969875
20	0.966633	0.674923	0.947166

local processing function described. The resulting image in this section was an image of uniformity and flatness. We then improved the contrast by enhancing the contrast of the image, improving the edges of the image (playing a role in determining the image better and determining the contrast of the image). The proposed method has been successfully developed; as evidenced in the simulation results, better results were obtained in the removal of vessels

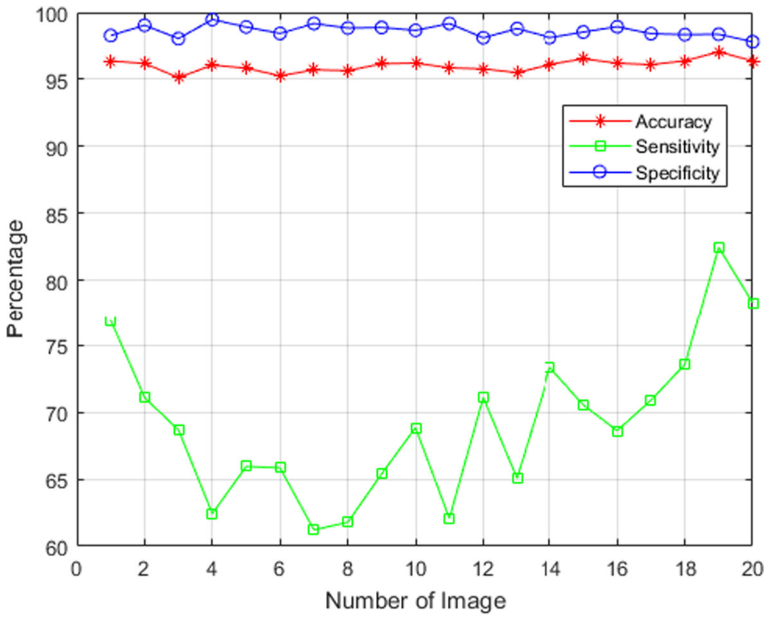

Fig. 16 Comparison of the result for DRIVE (test)

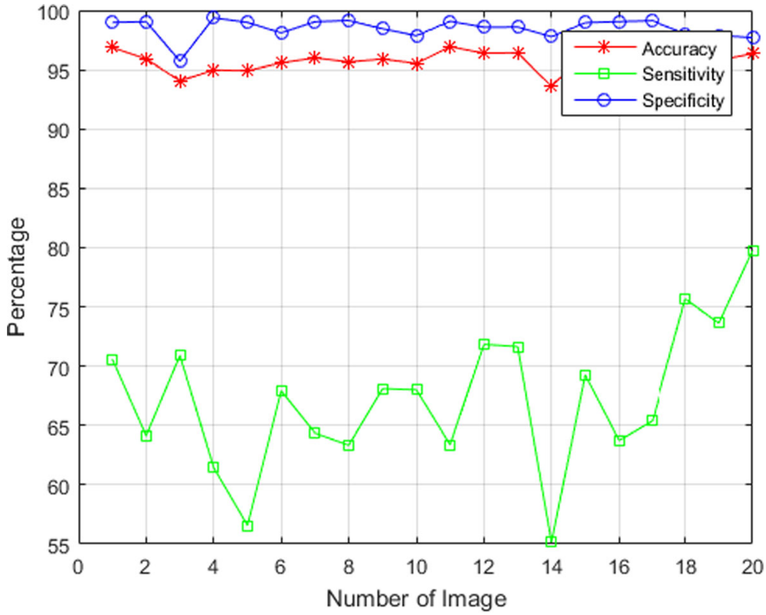

Fig. 17 Comparison of the result for DRIVE (train)

than in other methods. For future work, implementing the deep learning methods [4, 7, 13, 16] with proposed method may produce effective results. Combination of deep learning with proposed method extract properly the vessels from retinal fundus image and this extraction can help in diagnosis of diabetic retinopathy, hypertension, glaucoma diseases.

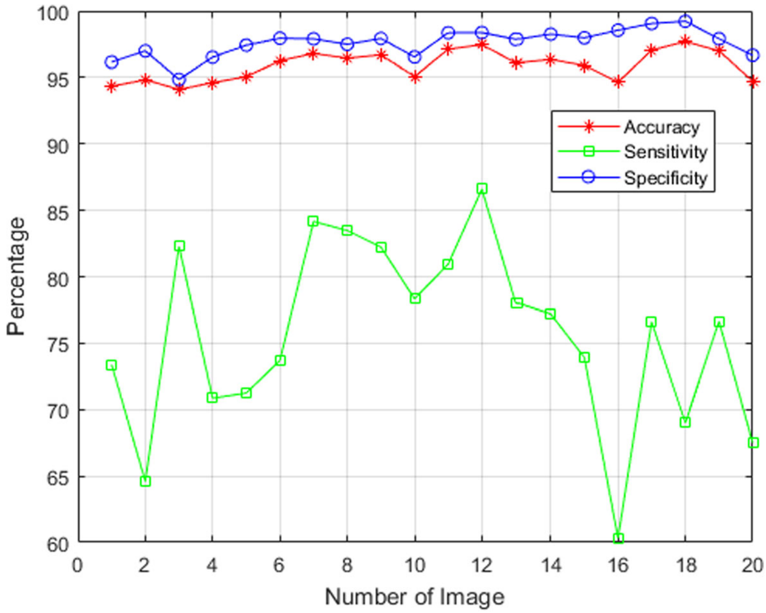

Fig. 18 Comparison of the result of STARE Database

References

1. Acharjya PP, Ghoshal D (2014) An image matching method for digital images using morphological approach. Int J Comput Electr Autom Control Inf Eng 8(5):859–863
2. Bhabatosh C (2011) Digital image processing and analysis. PHI Learning Pvt. Ltd
3. Fawcett T (2006) An introduction to ROC analysis. Pattern Recogn Lett 27(8):861–874
4. Feng Z, Yang J, Yao L (2017) "patch-based fully convolutional neural network with skip connections for retinal blood vessel segmentation," in 2017 IEEE International Conference on Image Processing (ICIP), IEEE, pp. 1742-1746.
5. Fraz MM, Remagnino P, Hoppe A, Uyyanonvara B, Rudnicka AR, Owen CG, Barman SA (2012) Blood vessel segmentation methodologies in retinal images–a survey. Comput Methods Prog Biomed 108(1):407–433
6. Ghoshal R, Saha A, Das S (2019) An improved vessel extraction scheme from retinal fundus images. Multimed Tools Appl 78(18):25221–25239
7. Guo S, Wang K, Kang H, Zhang Y, Gao Y, Li T (2019) BTS-DSN: deeply supervised neural network with short connections for retinal vessel segmentation. Int J Med Inform 126:105–113
8. Hoover A, Goldbaum M (2003) Locating the optic nerve in a retinal image using the fuzzy convergence of the blood vessels. IEEE Trans Med Imaging 22(8):951–958
9. Hoover A, Kouznetsova V, Goldbaum M (2000) Locating blood vessels in retinal images by piecewise threshold probing of a matched filter response. IEEE Trans Med Imaging 19(3):203–210
10. Hunt BR, Lipsman RL, Rosenberg JM (2014) A guide to MATLAB: for beginners and experienced users. Cambridge University Press, Cambridge
11. Kumbhar PG, Holambe S (2015) A review of image thresholding techniques. Int J Adv Res Comput Sci Softw Eng 5(6):160–163
12. Lam BS, Gao Y, Liew AW-C (2010) General retinal vessel segmentation using regularization-based multiconcavity modeling. IEEE Trans Med Imaging 29(7):1369–1381
13. Liskowski P, Krawiec K (2016) Segmenting retinal blood vessels with deep neural networks. IEEE Trans Med Imaging 35(11):2369–2380
14. Marín D, Aquino A, Gegúndez-Arias ME, Bravo JM (2011) A new supervised method for blood vessel segmentation in retinal images by using gray-level and moment invariants-based features. IEEE Trans Med Imaging 30(1):146–158
15. Nguyen UT, Bhuiyan A, Park LA, Ramamohanarao K (2013) An effective retinal blood vessel segmentation method using multi-scale line detection. Pattern Recogn 46(3):703–715
16. Oliveira A, Pereira S, Silva CA (2017) "Augmenting data when training a CNN for retinal vessel segmentation: How to warp?," In: 2017 IEEE 5th Portuguese Meeting on Bioengineering (ENBENG), IEEE, pp. 1–4.
17. Rahebi J, Hardalaç F (2014) Retinal blood vessel segmentation with neural network by using gray-level co-occurrence matrix-based features. J Med Syst 38(8):85
18. Raimondo F, Gavrielides MA, Karayannopoulou G, Lyroudia K, Pitas I, Kostopoulos I (2005) Automated evaluation of Her-2/neu status in breast tissue from fluorescent in situ hybridization images. IEEE Trans Image Process 14(9):1288–1299
19. Roychowdhury S, Koozekanani DD, Parhi KK (2015) Blood vessel segmentation of fundus images by major vessel extraction and subimage classification. IEEE J Biomed Health Inf 19(3):1118–1128
20. Saleh MD, Eswaran C (2012) An efficient algorithm for retinal blood vessel segmentation using h-maxima transform and multilevel thresholding. Comput Methods Biomech Biomed Eng 15(5):517–525
21. Staal J, Abràmoff MD, Niemeijer M, Viergever MA, Van Ginneken B (2004) Ridge-based vessel segmentation in color images of the retina. IEEE Trans Med Imaging 23(4):501–509
22. Tashfeen SH, Abrar A, Tondra TT (2017) Inflamed appendix detection from laparoscopic video footage using edge detection and morphological image processing. Dissertation, BRAC University
23. Wolf GW (1991) A Fortran subroutine for cartographic generalization. Comput Geosci 17(10):1359–1381
24. Zaini TRM, Jaafar M, Pin NC (2016) "H-minima transform for segmentation of structured surface". In: MATEC Web of Conferences, vol. 74: EDP Sciences, p. 00025.